Available online at www.sciencedirect.com

SCIENCE DIRECT®

Global and Planetary Change 43 (2004) 129–144

GLOBAL AND PLANETARY CHANGE

www.elsevier.com/locate/gloplacha

Low-frequency Atlantic sea level variability

G. van der Schrier[a,*], S.L. Weber[a], S.S. Drijfhout[a], J.A. Lowe[b]

[a] *KNMI, Department KS/VO, P.O. Box 201, De Bilt, 3730 AE, The Netherlands*
[b] *Hadley Centre, Department of Meteorology, The University of Reading, Early Gate, Reading, UK*

Received 9 September 2003; received in revised form 26 March 2004; accepted 29 March 2004

Abstract

The control run of the Hadley Centre-coupled climate model (HadCM3) is used to establish the sources of multidecadal/centennial sea level (SL) variations in the northwest Atlantic. It is shown that variations in the sea level for the largest part of this area are related to variations in the thermohaline structure of the upper (≈ 500 m) part of the ocean. Temperature variations dominate steric sea level variations, while salinity variations are dominant only in the margins of the Labrador Sea and near the Mediterranean outflow. In the Labrador Sea, lower layers in the ocean also contribute to the variability in expansion/contraction of the water column. It is shown that along the North American East Coast, variations in the thermohaline structure of the water column are predominantly related to variations in the wind-driven circulation rather than the thermohaline circulation, which dominates the thermohaline structure in the central parts of the North Atlantic. In the Gulf Stream area and near the Labrador Current, sea level has on the multidecadal/centennial time scale a strong barotropic signal superposed on steric sea level variations.

Keywords: Sea level; North Atlantic; Ocean circulation; Climate modelling

1. Introduction

Several reconstructions of the North Atlantic coastal sea level (SL) have become available recently. These records are based on foraminiferal analysis of peat cores from tidal wetlands, most of them from the eastern seaboard of North America. Some of these records extend over 1500 years back in time and show rapid and frequent fluctuations in sea level on the multidecadal to centennial time scale. These long sea level reconstructions allow future sea level variations to be placed in a historical context (Church et al., 2001), but the typical temporal resolution of these records varies between 50 and 150 years, making them effectively low-pass filters. A review of recently published reconstructions of late Holocene sea level change is given by Long (2000). Despite the increase in available reconstructions of past sea level, the source for low-frequency sea level variations remains obscure, as is a possible connection to climate in the North Atlantic region. A variety of mechanisms have been suggested in the literature regarding the source for multidecadal/centennial North American coastal sea level variations. It is hypothesised: (1) that variations in the sea level from Wolfe Glade (DE, USA)

* Corresponding author. Current address: Climatic Research Unit, University of East Anglia, Norwich, UK. Tel.: +44-1603-592318.
E-mail address: g.schrier@uea.ac.uk (G. van der Schrier).

0921-8181/$ - see front matter © 2004 Elsevier B.V. All rights reserved.
doi:10.1016/j.gloplacha.2004.03.001

reflect a spin-up and slow down of the Gulf Stream, responding in its turn to variations in the wind field (Fletcher et al., 1993); (2) or that reconstructed sea level fluctuations from the Gulf of Maine (USA) reflect variations in temperatures in eastern North America (Gehrels, 1999; Gehrels et al., 2003). Reconstructed sea level fluctuations from Long Island Sound (CT, USA); (3) have been linked to surface air temperature variations over the northwest Atlantic (van de Plassche, 2000). Recently, (4) Crowley et al. (2003) interpret this latter reconstruction, based on a study with an Energy Balance Model, as a reflection of ocean heat content changes, which are related to Northern Hemisphere surface temperature variations. Finally, (5) van de Plassche et al. (2003) relate this reconstruction, and another reconstruction from Farm River marsh (CT, USA), to low-frequency variations in the deep-ocean hydrography, which expand or contract the water column. This latter hypothesis is based on results of an intermediate complexity General Circulation Model (GCM; van der Schrier et al., 2002). There is evidently a rich variety in hypotheses for the source for low-frequency sea level variations along the North American eastern seaboard.

The aim of this study is to determine the mechanisms for multidecadal/centennial sea level variations from 1000 years of data from the state-of-the-art Hadley Centre-coupled climate model (HadCM3), which could provide a framework for the interpretation of sea level reconstructions. The time scales and time span of interest here reflect the temporal resolution and length of the proxy records for sea level, which are typically multidecadal/centennial and 1000 years, respectively, but all conclusions reached in this study are based on a model simulation. A comparison of some sort with the actual proxy records for sea level is beyond the scope of this paper. The main focus of this paper is low-frequency sea level variations along the northeastern seaboard of North America.

The significance of using the Hadley Centre-coupled climate model (HadCM3) for this study relates to its high spatial resolution in the ocean component, both horizontally ($1.25° \times 1.25°$) and vertically (20 unevenly spaced levels, of which half are in the upper 360 m). Furthermore, the parameterisations of, e.g., subgrid scale processes have a much higher degree of realism than that of models used so far for modelling multidecadal/centennial sea level. On the other hand, output from even more realistic models than HadCM3 is unsuitable for this study because the length of simulations of these latter models are currently limited to only a few decades.

Despite the high spatial resolution of HadCM3, a realistic representation of processes will become more and more inadequate further up the continental shelf towards the highly irregular, and therefore badly resolved, coastline. However, an earlier study (Noble and Gelfenbaum, 1992) concludes that sea level variations remain highly coherent across the shelf, up to the shelf break into the deep ocean, validating the use of a General Circulation Model (GCM) in sea level studies.

This study is organized as follows: Section 2 gives a brief description of the model, and in Section 3, sea level variations and the role of hydrographic changes therein are presented. In Section 4 the sources for low-frequency sea level variations in selected regions are presented, and this study is summarized and discussed in Section 5.

2. Model description

The HadCM3-coupled ocean–atmosphere–sea ice general circulation model is developed at the Hadley Centre for use in climate studies. Given the complexity of the model, only a brief summary of its description is included here; it has been described in detail by Pope et al. (2000) and Gordon et al. (2000), where also a validation of some climate parameters is given. Here, only a brief summary of the model's description is given. The atmospheric component has a horizontal grid resolution of $2.5° \times 3.75°$ and 19 vertical levels using a hybrid coordinate. The ocean component has a horizontal resolution of $1.25° \times 1.25°$, and the 20 vertical levels are unevenly spaced to increase resolution near the ocean surface. Ten levels are found in the upper 360 m. The sea–ice model uses a simple thermodynamic scheme and contains parameterisations of ice drifts and leads.

The HadCM3 model is a 'rigid-lid' model in which the ocean conserves volume (rather than mass) and has a flat surface. In this model, sea level can be deduced indirectly, as described in the Appendix, or more exhaustively by Gregory et al. (2001).

The control run suffers from a monotonous change in the hydrography over the entire simulation (a trend), which decreases for the upper ≈ 1000 m faster than for the deeper part (Gordon et al., 2000, Fig. 3a and b). To avoid the largest trend-related changes which could cloud the analysis, we used the latter 1000 years of the 1700-year-long control run. Furthermore, temperature and salinity data below ≈ 1000 m are nonlinearly detrended by subtracting a third-order polynomial. This removes any linear trend and variability with the longest (millennial) time scales, which is expected to be related to model adjustments rather than to real physical phenomena.

3. Hydrography and sea level of the North Atlantic

We concentrate in this study on the sea level variability during winter (December–January–February, DJF). Sea level in the North Atlantic in the cold season is more energetic than that in the warm season. This is related to a more energetic atmosphere and larger ocean–atmosphere buoyancy and momentum fluxes in this season (Schmitt et al., 1989; Charnock, 1994).

A large part of the statistical analysis in this study is based on (ordinary Pearson) correlations. The correlations r are significant at the 95% level in a standard two-sided t-test for $n=25$ independent samples, if the inequality $|r| \geq 0.4$ holds. For a standard one-sided test this is $r \geq 0.34$. The number n is obtained as the length of the simulation divided by the filter period of 40 years.

Sea level variations can be brought about by variations in atmospheric pressure, or the 'inverted barometer effect', variations in wind stress and changes in steric sea level. In areas with low atmospheric pressure, the sea surface is higher and vice versa. Furthermore, changes in wind stress exerted on the ocean surface will change the Ekman transport, convergences or divergences will develop and the sea level pattern will change. Finally, the steric sea level is high when the water is warm, low when it is cold. Conversely, a high steric sea level corresponds to a low value of salinity. Steric sea level is defined as the geopotential thickness of the entire water column and is computed diagnostically from the hydrography of the water column. The unit of geopotential thickness is chosen such that a change in geopotential thickness of 1 dyn cm $\equiv 1000$ cm^2 s^{-1} corresponds to a change in geometric thickness of approximately 1 cm (Levitus, 1990). Steric sea level (or geopotential thickness) is computed relative to a standard ocean having homogeneous temperature and salinity of 0 °C and 35 psu, respectively. Mass changes of mountain glaciers and ice sheets are of importance for sea level variations but are excluded in this study.

First it is shown that multidecadal sea level variations in the largest part of the North Atlantic are dominated by variations in steric sea level. The sources of variations in sea level can be distinguished by their frequency characteristics. The average of the spectra of all grid boxes, that is, the averaged spectrum, of North Atlantic atmospheric pressure variations has its energy more or less evenly distributed over the range of possible frequencies. For frequencies higher than 0.2–0.3 cycles year^{-1}, they are comparable or stronger than variations in sea level due to steric sea level or wind stress-related sea level variations. On a multidecadal time scale however, sea level changes due to sea-level pressure (SLP) fluctuations are insignificant compared to the other sources. In this study, we will therefore define sea level (SL) as the composite of sea level variations related exclusively to variations in wind stress (and which would also occur in a barotropic ocean) and sea level variations due to variations in the hydrography of the water column (the steric sea level).

The averaged spectra over the Atlantic of steric sea level and SL are very similar. This indicates that on average over the North Atlantic ocean, variations in SL are dominated by variations in the steric sea level (not shown). This is also reflected in a simple correlation analysis where for each grid box, variations in sea level are correlated with those in steric sea level. The averaged correlation (over the area 20–75°N, 85°W–15°E), that is the correlation in each grid box averaged over this area, increases to about 0.66 when the data are low-pass-filtered, removing frequencies higher than 0.1 cycle year^{-1}. The averaged correlation remains approximately constant when stronger filters are used. To focus on multidecadal/centennial sea level variability, a low-pass filter is applied, which removes oscillations with periods smaller than 40 years. Fig. 1 shows the correlation map between SL and steric sea level for this low-pass filter. The correlations are

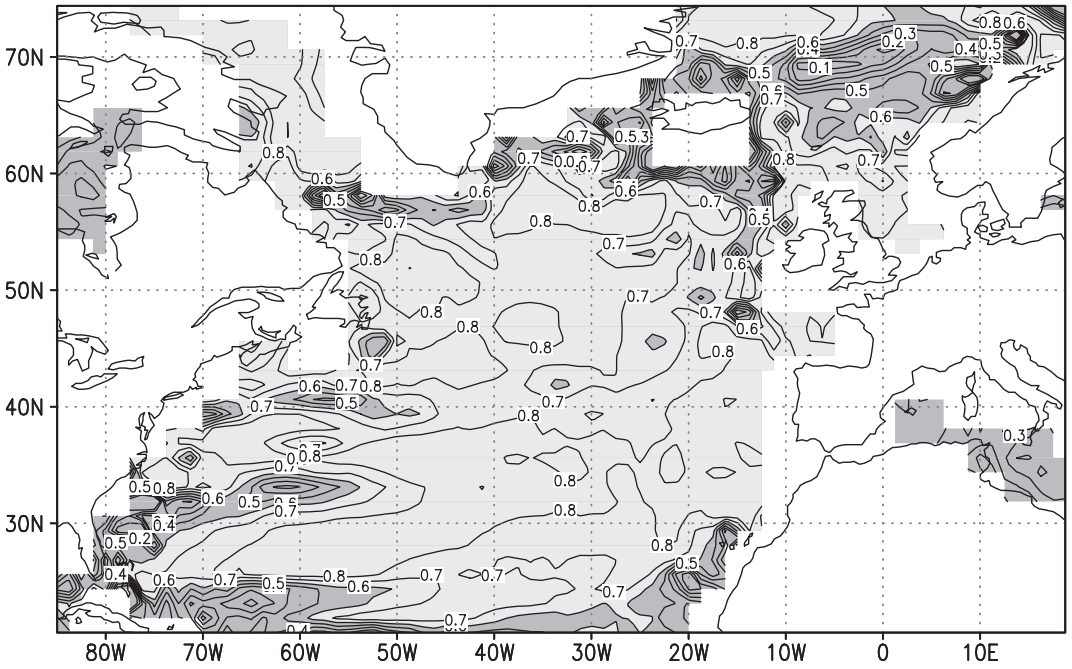

Fig. 1. Correlation between sea level and steric sea level for each grid box (low-pass-filtered, 40 years). Correlations are generally very high, except near Iceland and in the GIN Sea. Also near the eastern seaboard of the United States, small areas of low correlations are found. Areas with correlations ≤ 0.6 are dark grey. Correlations ≥ 0.4 are statistically significant at the 95% level.

generally very high, except those around Iceland and in the Greenland–Iceland–Norway (GIN) Sea; also, near the United States East Coast and in the Labrador Sea localized areas, with low (≤ 0.6) to statistically insignificant correlations are seen.

Variations in the steric sea level can be thought of as being composed from variations in geopotential thickness of successive subsurface layers. Averaged over the North Atlantic, the top ≈ 500 m contribute most to the variability of steric sea level (Fig. 2). The deep ocean fails to contribute significantly to North Atlantic averaged steric sea level variability in this simulation on all time scales including multidecadal/centennial time scales. A lack of variation in the geopotential thickness of the deep ocean does not imply that potential temperature and salinity do not experience fluctuations; there is considerable variation in 'spiciness' (Flament, 2002), a state variable which is largest for hot and salty water. Spiciness variations are dynamically neutral in the ocean by virtue of the density compensation of temperature and salinity anomalies. However, other regions in the North Atlantic realm are characterized by comparable amounts of energy in surface and subsurface geopotential thickness fluctuations, like the Labrador Sea and the GIN Sea. The dominance of the geopotential thickness of the upper ≈ 500 m on steric sea level is the motivation to adhere to this upper layer higher interest than to lower layers.

An Empirical Orthogonal Function (EOF) analysis shows that the first leading mode (first EOF) of sea level variability has its largest amplitude covering the area of Cape Hatteras downstream on the path of the North Atlantic Current (NAC). This mode accounts for 18.8% of the total variance and captures variability in the strength of the Gulf Stream (Fig. 3a). The second mode, accounting for 11.8% of the total variance (and well separated from the remaining modes, which each explain less than 6%), has an amplitude maximum south of the mean position of the model's Gulf Stream and an amplitude minimum north of it, covering an area from the northeast of the United States into the Labrador Sea and extending nearly to the European continent (Fig. 3b). This mode can be associated with variations in the position of the Gulf Stream. The spectra of the time evolution of these EOFs, or

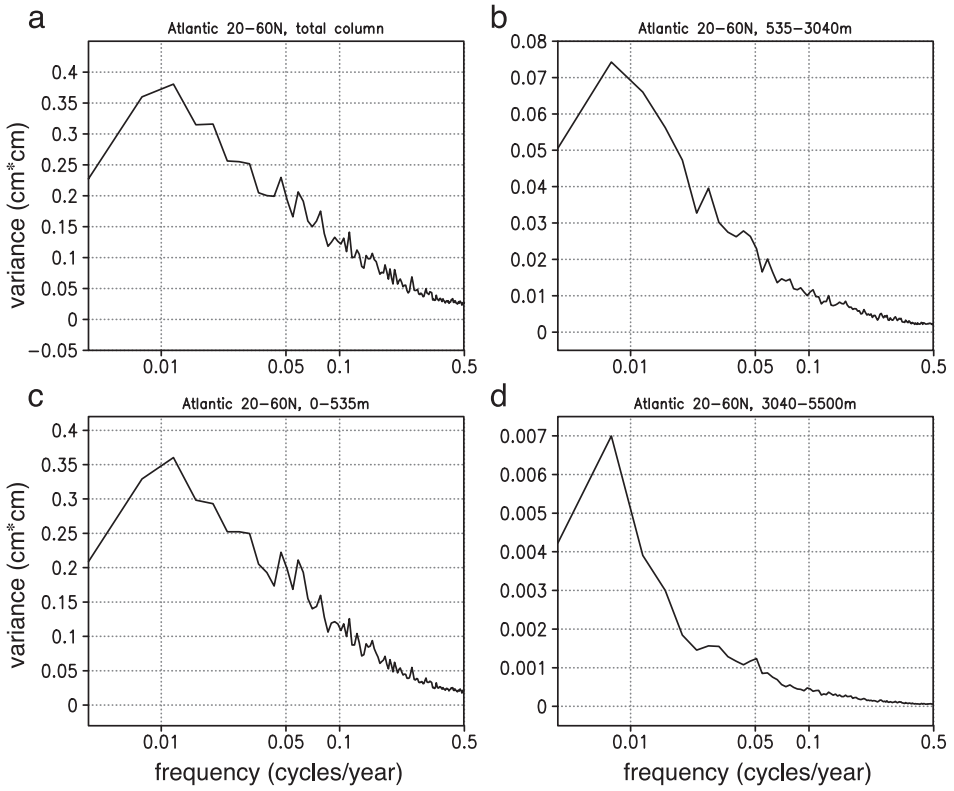

Fig. 2. Averaged spectra over the North Atlantic for steric sea level (a) and the contributions from three successive subsurface layers. Note the change in vertical scale.

Principal Components (PC), shows that the leading mode of sea level variability has a significant peak (at the 95% level) near 0.15 cycles year^{-1} (Fig. 3c). The second most important mode has a significant peak at multidecadal periods (Fig. 3d) and explains the multidecadal peak in Fig. 2a and c.

The importance for temperature or salinity variations in fluctuations of steric sea level is assessed by computing the contributions of temperature and salinity to geopotential thickness by substituting the standard value of 35 psu for salinity in the former and 0 °C for temperature in the latter case. The geopotential thickness of the upper 535 m (corresponding to the upper 11 layers) is computed and correlated with the corresponding grid box of geopotential thickness due to temperature variations only and geopotential thickness due to salinity variations only (Fig. 4). For the upper 535 m holds that the correlation maps are approximately complementary to each other with dominance of salinity east of Greenland, in the Labrador Sea and Baffin Bay extending around Newfoundland to Nova Scotia. Near the outflow of the Mediterranean, salinity also dominates. The temperature signal dominates geopotential height of the upper 535 m in the western and central subtropical gyre and along the path of the Gulf Stream/North Atlantic Current (NAC) system.

These observations change dramatically in the northwest Atlantic when geopotential height of the upper 3040 m (upper 16 layers) is considered, roughly including the model's North Atlantic Deep Water (NADW). The dominating influence of salinity on geopotential thickness variations is now limited to the margins of the Labrador Sea and along the coasts of Newfoundland and Nova Scotia. In the deeper parts of the Labrador Sea, temperature variations are seen to play a more profound role. We will return to this in Section 4.3.

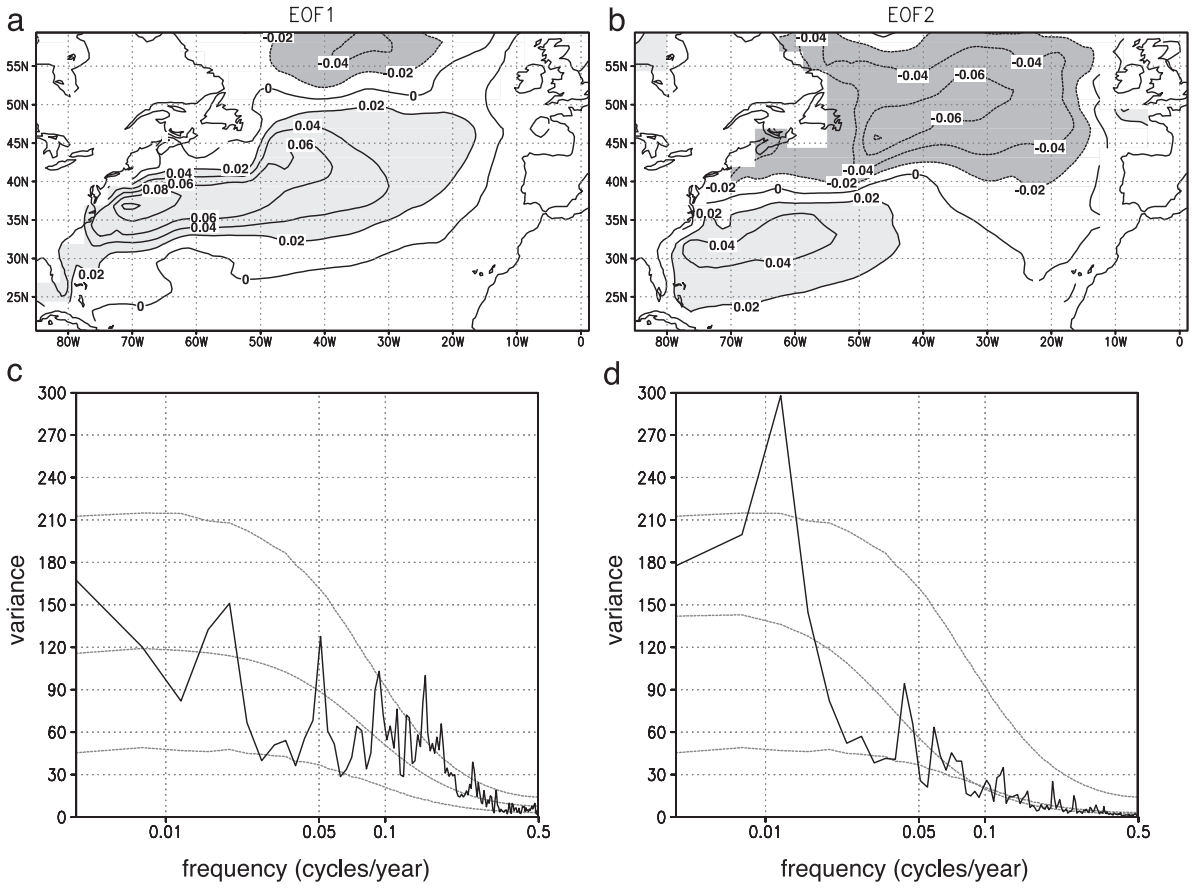

Fig. 3. The first (a) and second (b) leading modes in sea level variability, explaining 18.8% and 11.8%, respectively, of the total variance. The spectrum of the first leading mode (c) shows a significant peak at ≈ 0.15 cycles year^{-1}, while the second leading mode has a significant peak at multidecadal periods. The 95% confidence levels are drawn in gray.

In the remainder of the North Atlantic, little changes in the respective roles of salinity and temperature. This is a reflection of the dominance of the geopotential height of the upper ≈ 500 m on steric sea level.

A clear dominance of either temperature or salinity between 40°N and 45°N near the American coast, home of several sea level reconstructions, is absent in this simulation.

4. Sources for low-frequency sea level variations in different areas of the North Atlantic

We will now turn to the processes which are reflected in low-frequency sea level variations. Here we focus on localized areas within the North Atlantic, the choice of which is motivated by a combination of the analysis of Section 3 and the place of origin of some sea level reconstructions.

4.1. Sea level in the Gulf Stream region

Variability in the steric sea level in the Gulf Stream region is strongly correlated with temperature variations of the upper part (0–535 m) of the ocean; steric sea level simply acts here as a proxy for heat content. Changes in steric sea level in areas directly hugging the coast are, in its turn, closely related to advection of heat. The importance of the advective heat flux for the heat content of the upper part of the ocean is corroborated by comparing, for each col-

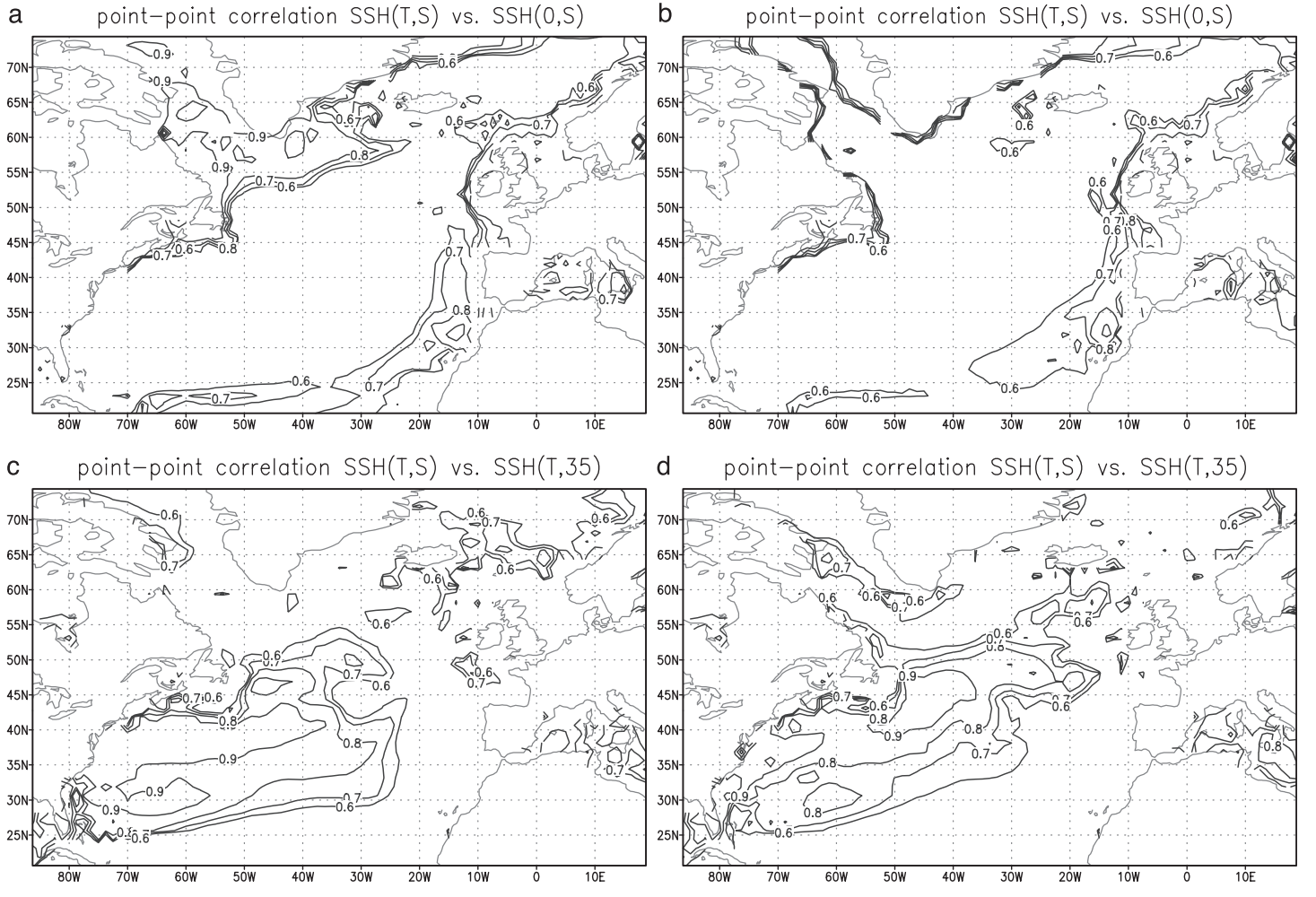

Fig. 4. Correlation of geopotential height of the upper 535 m (left) and the upper 3040 m (right) with the contribution of salinity variations only (a and c) and temperature variations only (b and d). The correlation maps are consistent with dominance of salinity east of Greenland, in the Labrador Sea and Baffin Bay extending to Newfoundland. Isolated patches where salinity variations dominate steric sea level changes are found in the eastern and western subtropics. Temperature dominates in the western and central subtropical gyre and along the path of the Gulf Stream/NAC system.

umn of grid boxes extending to the bottom, the volume integrated net advective heat flux with the surface integrated ocean–atmosphere net heat flux. Both the surface heat flux and the volume-integrated net advective heat flux over a column of grid boxes supply/extract heat to expand/contract this column. For the grid boxes along the path of the Gulf Stream extending into the central North Atlantic and in the slope water north of the Gulf Stream, the variability in the advective heat flux is an order of magnitude larger than the surface-flux-related quantity with maximum values south of Cape Hatteras. Farther offshore in the subtropical North Atlantic, variability in the advective and surface heat fluxes is comparable (Fig. 5).

Variations in meridional heat transport are related to both variations in the Meridional Overturning Circulation (MOC) and variations in the wind-driven circulation. To illustrate this, the dominant patterns of variability in the MOC and the horizontal stream function are constructed using an Empirical Orthogonal Functions (EOF) computation. The most dominant pattern, or first EOF, of the low-pass-filtered (40 years) MOC explains 49.3% of the variance and spans the entire North Atlantic. This pattern reflects an increase or decrease of the entire North Atlantic Deep Water (NADW) cell (Vellinga and Wu, submitted for publication). The first EOF of the low-pass-filtered (40 years) horizontal stream function explains 35.3% of the variance and represents increase/decrease in the strength of the wind-driven circulation. The time evolution of these EOFs, the Components (PC), are correlated with low-pass-filtered (40 years) meridional heat transport (Fig. 6). It shows that near 25°N, both the MOC and the horizontal stream function are highly correlated with meridional heat transport. For latitudes north of $\approx 35°$N, the correlation between meridional heat transport and the PC of the first EOF of the horizontal stream function is clearly higher than the correlation with the PC of the first EOF of the MOC.

Overall, variations in the horizontal stream function determine to a large degree variations in the steric sea level in areas near the United States East Coast. This can also be concluded from the following: a correlation between steric sea level and the horizontal stream function, both averaged over 30–40°N, 80–70°W, yields 0.51, while steric sea level and the PC of the first EOF of the overturning fail to have a statistically significant correlation at 0.20 (low-pass filter, 40 years).

Fluctuations in steric sea level explain a large part of sea level variability, but variations in large-scale wind stress curl also contribute to SL variability as they determine the strength of the subtropical and subpolar gyres. This is shown in Fig. 7, where steric sea level and horizontal stream function are multiply regressed on SL. Each field is first standardized with its (local) standard deviation, and then regression coefficients α and β are determined so that steric sea level, scaled by α, and the horizontal stream function, scaled by β, optimally explain (in a least-squares sense) SL over 1000-year data. In Fig. 7a, the coefficient α is, averaged over this region, 0.71, with maxima in the subtropical and subpolar gyres. Minima are found roughly along the path of the Gulf Stream/NAC system, where conversely, the coefficient β has its maxima. Both fields combined explain nearly all variability in SSH. The data is low-pass-filtered (40-year filter).

In conclusion, SL in the Gulf Stream region is determined in large part by variations in the steric sea level, but approximately along the path of the Gulf Stream/NAC system variations in large-scale wind stress curl contribute significantly. Moreover, low-frequency steric sea level along the eastern seaboard of the United States and in the strong advective regimes of the Gulf Stream/NAC system is related to divergences in the advective heat flux, while ocean–atmosphere heat flux variability paces heat content only in the stagnant water masses of the subtropical gyre.

The advective heat transport in the ocean can be decomposed in a gyre and overturning component. However, uniquely identifying the gyre component with the wind-driven circulation is inappropriate (Saenko et al., 2002). This is because in the absence of wind forcing, there remains a gyre component due to the thermohaline circulation. Nevertheless, variations in the gyre circulation are highly correlated with variations in the wind field. A correlation analysis of low-pass (40 years) filtered horizontal stream function (20–50°N, 85–40°W) and the PC of the first EOF of the zonal wind field (explaining 62.6% of the variance) yields correlations up to 0.85

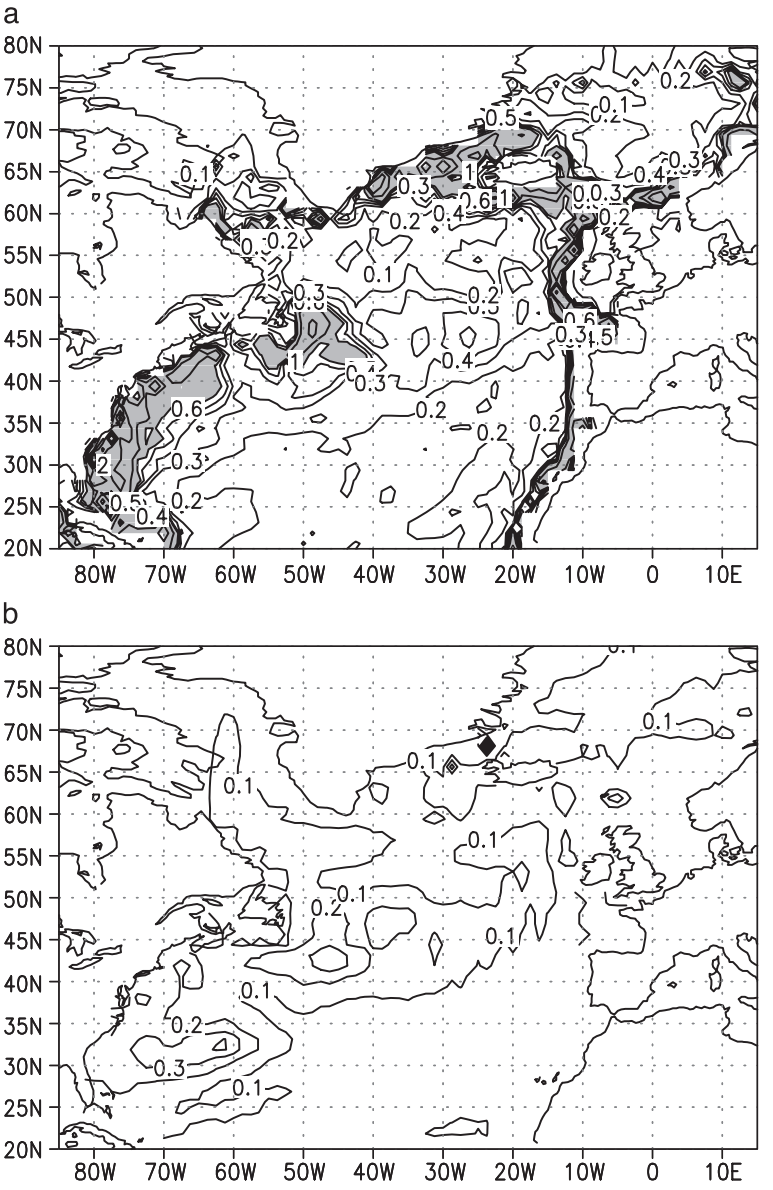

Fig. 5. Standard deviation of the net advective heat flux, integrated over a column of grid boxes over the upper 535 m (11 layers) of the model (a) and the standard deviation of the surface integrated net heat flux into this column of grid boxes (b). The fields have been low-pass-filtered with a 40-year filter. Values are in units of 10^{12} W, and values larger than 1.0 are gray. Contour intervals are 0.1 for values below (and including) 0.6, while for values higher than 1.0, the contour interval is 1.0.

in the central part of this domain. The correlations were much lower over areas with gradients in the bathymetry, where changes in the density gradient will also be reflected in changes of the horizontal stream function.

4.2. Slope water sea level

The leading mode, or first EOF, of the model low-pass-filtered (40 years) sea level variability in the region 20°N–50°N, 85°W–40°W (Fig. 8) has its

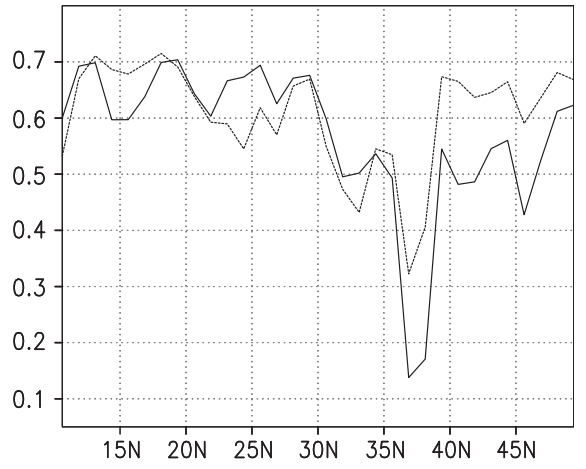

Fig. 6. Correlation between the principal component of the first EOF of the meridional overturning circulation (explaining 49.3% of the variance) and meridional heat transport (solid line), and the principal component of the first EOF of the horizontal stream function (explaining 35.3% of the variance) and meridional heat transport (broken line) as a function of latitude. All fields are low-pass-filtered (40 years).

largest amplitude covering the area near Cape Hatteras, just south of where the Gulf Stream leaves the coast. Large amplitudes continue downstream along the path of the NAC. There is an opposing amplitude south of the Gulf Stream, but this dominant mode fails to have any significant impact on the sea level north of the Gulf Stream. This first mode accounts for 45.3% of the sea level variability. The second most dominant pattern of sea level variability (second EOF) accounts for 25.0% of the variance and is well separated from the remaining patterns (each accounting for less than 8.5%). The second EOF has its largest amplitude north of the Gulf Stream, increasing northward along the coast into the subpolar gyre. This pattern represents the north- and southward shifting of the position of the Gulf Stream. It is this pattern which largely determines sea level variability of the slope water.

A correlation map between SL and the principal component of the second EOF has similarities to this EOF pattern with correlations along the coast north of 42 °N between 0.6 and 0.7 (Fig. 9), indicating that the north/southward shifting of the position of the Gulf Stream indeed determines SL in this region. The correlation between the PC of the second EOF of SL and the geopotential height of the upper 535 m due

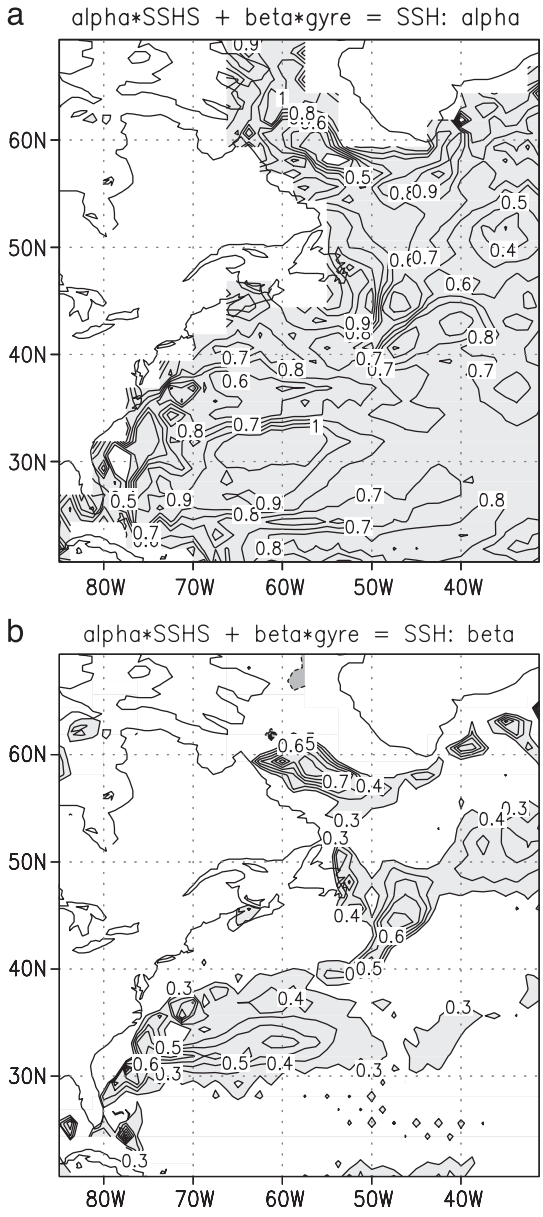

Fig. 7. Coefficients α (a) and β (b) which optimally (in a least-squares sense) explain sea level in a multiple regression analysis, using the steric sea level field and the horizontal stream function. The steric sea level field is seen to dominate sea level almost everywhere, except along the path of the Gulf Stream/North Atlantic Current, where the horizontal stream function is important. Normalized anomalies are used, so that the values of α and β can be compared.

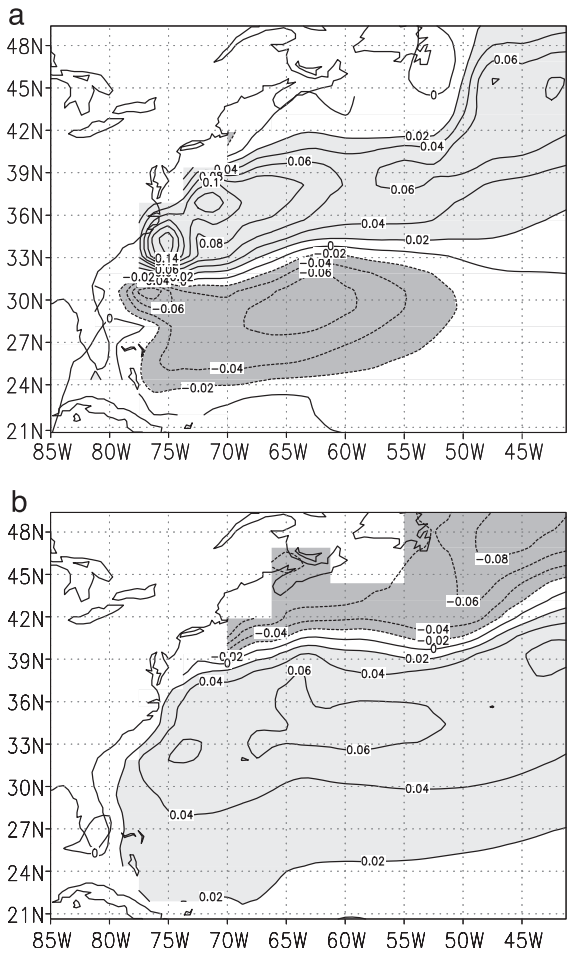

Fig. 8. First and second EOF of low-pass-filtered (40 years) sea level. The first EOF has its largest amplitude long the path of the Gulf Stream/NAC system and account for 45.3% of sea level variability. The second accounts for 25.0% of the sea level variability and represents a north- and southward shifting of the position of the Gulf Stream.

to temperature variations only is, in this region, ≈ 0.5–0.6. This indicates that a change in water mass characteristics associated with the changes in the Gulf Stream's position is largely responsible for sea level change.

The separation point of the Gulf Stream in this model is too far north (Cooper and Gordon, 2002), which suggests that the size of the region where sea level is under control of shifts in the position of the Gulf Stream may be underestimated.

4.3. Sea level in the Labrador Sea

Low-frequency geopotential height of the upper 535 m in the Labrador Sea correlates very strongly with geopotential height due to salinity variations only (correlations are in large areas 0.8/0.9; Fig. 4a). However, this ceases to be valid when steric sea level (geopotential height of the entire water column) is considered. High correlations between steric sea level and its salinity-related variability are only found near the margins of the Labrador Sea, extending southward along the coasts of Newfoundland and Nova Scotia. In the interior of the Labrador Sea, temperature variations dominate variations in steric sea level (correlations ≈ 0.6/0.7; Fig. 4d).The reason for this change in character of expansion/contraction of the water column with the length of the water column is twofold. Salinity anomalies in the deeper layers are out-of-phase or uncorrelated to those in the upper layers, neutralizing or hiding the salinity-related signal of the upper layers in steric sea level. This seems to be in agreement with the analysis of Houghton and Visbeck (2002).Temperature variations in the upper and deeper layers oscillate much more in concert, explaining the importance of the temperature-related steric sea level signal. The consequence of this is that salinity anomalies in the upper part of the Labrador Sea are not reflected in steric sea level, except near the margins of the Labrador Sea. This is in agreement with the findings of Curry and McCartney (2001), who conclude that the occasional salinity anomalies in the subpolar gyre contribute relatively little to the Labrador Basin potential energy anomaly; a quantity that is related to steric sea level.

A tentative explanation for this is that apparently convection mixes the salinity anomaly of the upper to the deeper layers, reducing the salinity anomaly in the upper layer and establishing one in the deeper layers. During deep convection, water at depth is mixed with cold water from the upper layer while any heat gain of the upper layer is quickly lost to the atmosphere due to the vigorous ocean–atmosphere heat exchange.

Fig. 1 shows that in the Labrador Sea between 55°N and 60°N and along the western margin, the correlation between steric sea level and sea level is relatively low. This is an indication that in this region SL has a strong barotropic component. The Labrador Current flowing south along the Labrador coast has

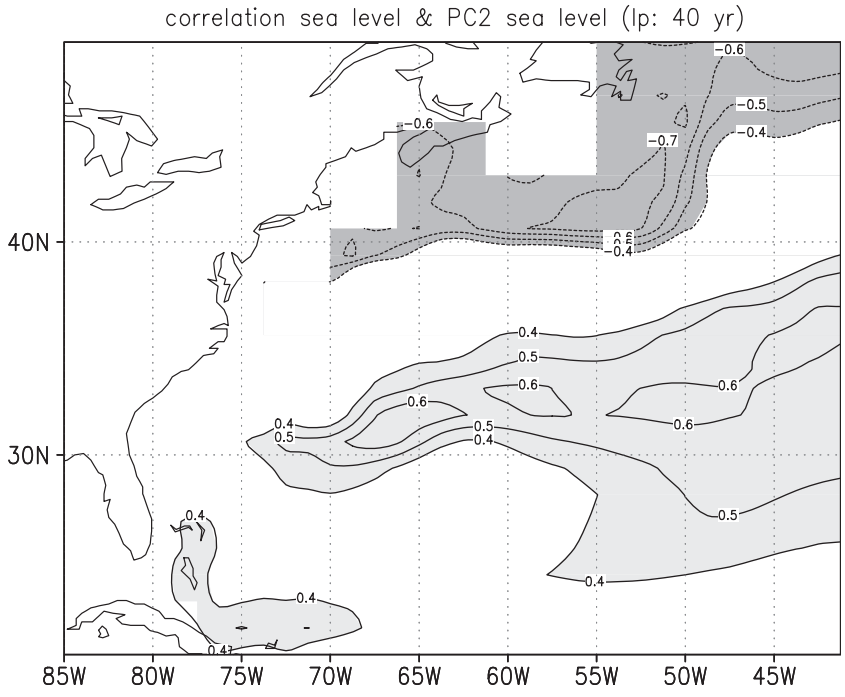

Fig. 9. Correlation sea level with the principal component of the second EOF of sea level, which reflects a north- and southward moving of the Gulf Stream position. The (absolute) correlations along the North American coast, north of 42°N, are between 0.6 and 0.7 (40 years, low-pass-filtered).

indeed a strong barotropic component; the standard deviation of the horizontal stream function at 60°N is only slightly smaller than that of the total zonally- and vertically-averaged southward volume transport at 60°N between Greenland and the Labrador coast.

Sea level in the Labrador Sea, especially along the western margin, is related both to changes in the hydrography and to changes in the wind-driven circulation. Despite of this complexity, sea level in the Labrador Sea can be related to an important climate parameter. A correlation analysis indicates that multi-decadal sea level variations reflect variations in the North Atlantic meridional overturning circulation (Fig. 10), with maximum correlations of 0.6–0.7 in the central subpolar gyre and the northern parts of the Labrador Sea and minimum correlation of -0.7 just south of the model's Gulf Stream. A similar dipole structure was retrieved when meridional heat transport at 25°N was correlated with steric sea level. This correlation pattern echoes the relation between the concept of a baroclinic pressure gradient and a transport index as put forward by Curry and McCartney (2001). The area between the maximum and minimum correlations is exactly aligned to the climatological mean path of the Gulf Stream/NAC system of the model.

4.4. Sea level and the Mediterranean outflow

Sea level variations in the Atlantic hugging the North African and Spanish coast are seen to be dominated by variations in salinity (Fig. 4). This is related to the Mediterranean outflow. The parameterisation, which describes this outflow, simulates the exchange of temperature and salinity in the upper $\approx$ 1195 m (Gordon et al., 2000). The rate of change of the tracer field at each level is parameterised as a relaxation to an average value composed of grid boxes in the Mediterranean and the Atlantic, which are directly adjacent to the Straits of Gibraltar. East of the Straits of Gibraltar, the Mediterranean temperatures are lower than those in the Atlantic side of the Straits of Gibraltar to a depth of $\approx$ 900 m, while salinities at the Mediterranean side and over the

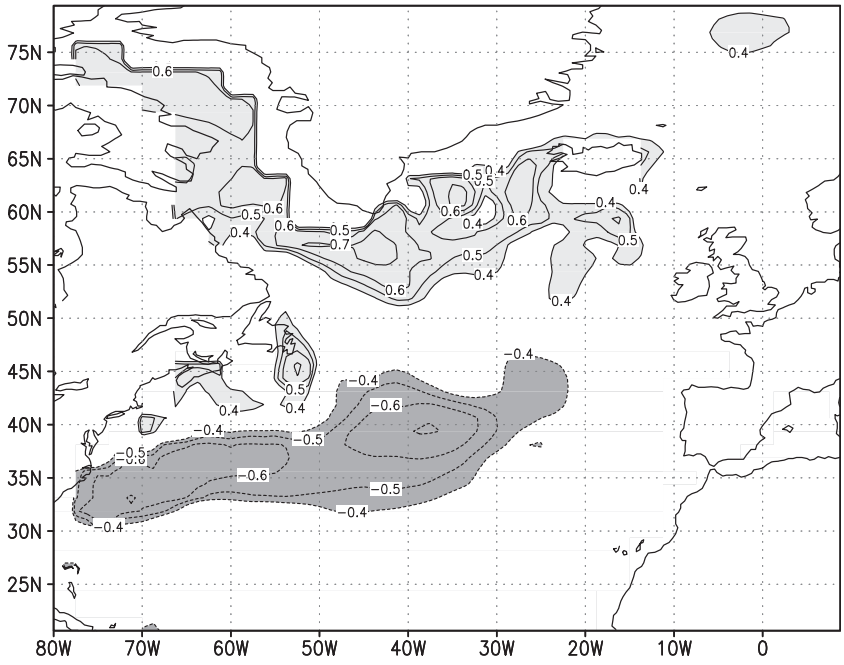

Fig. 10. Correlation of the first EOF of the meridional overturning circulation with sea level. Data is low-pass-filtered (40 years).

complete water column are much higher than those at the Atlantic side. The variability in Mediterranean temperatures, measured in terms of standard deviation over 1000 years, is over the complete column less than that of the Atlantic. In contrast to this, variations in Mediterranean salinities are larger than those in the Atlantic. The effect of the parameterisation is that the Atlantic temperatures (in the upper $\approx$ 900 m) are decreased while variations in temperatures are damped, and the average level of Atlantic salinity increases while its variability is enhanced. The combination of these two effects results in a more dominant role of salinity in density variations at the expense of temperature.

5. Summary and Discussion

The sources for multidecadal/centennial sea level variations in the North Atlantic ocean are investigated using 1000 years of the control simulation of the Hadley Centre coupled climate model (HadCM3). The analysis shows that steric sea level, the expansion/contraction of the water column due to variations in temperature and salinity, is on average over the North Atlantic, the most important contributor to sea level variations. Localized areas exist however where sea level variations relate most strongly to wind field variations. Steric sea level fluctuations are dominated by variations in the geopotential height of the upper $\approx$ 500 m. The deep ocean (below $\approx$ 500 m) hardly contributes to variations in steric sea level. Exceptions are areas as the Labrador Sea, where a strong vertical exchange of water occurs. The amount of energy in the geopotential thickness of the upper and deeper parts of the ocean is comparable in this region. On a multidecadal time scale, sea level changes due to changes in sea-level pressure fluctuations are found to be insignificant compared to steric sea level variations or variations in sea level due to variations in the wind field. An analogous conclusion has been reached earlier by Gregory et al. (2001).

By comparing data from tide gauges and historical hydrographic observations, Levitus (1990) observes that interpentadal changes (changes in a pentad, or 5-year period) in steric sea level are generally consistent with observations of sea level in the subtropical and western subpolar gyres. This gives additional credit to

dominance of steric sea level as a contributor to sea level variations.

Fluctuations in steric sea level are almost everywhere dominated by variations in temperature, with the exception of the margins of the Labrador Sea up to Newfoundland and the Mediterranean outflow region, where salinity is found to dominate steric sea level variability.

The minor role of the deep ocean in the variability of steric sea level is in contrast to results found earlier by van der Schrier et al. (2002), based on an analysis of an intermediate complexity GCM. In the current analysis, it is found that below $\approx$ 500 m, geopotential thickness hardly varies due to density compensation of temperature and salinity anomalies. Density compensation in the deep ocean is not found in the simpler model, where geopotential thickness was dominated by variations in deep-ocean salinity. The salinity-related variations in deep-ocean geopotential thickness in the northern North Atlantic (north of 60°N) in the simpler model and in the current model amount to $\approx \pm 3$ cm. The amount of variability in deep-ocean temperatures differs in the models.

van de Plassche et al. (2003) argue, based on further simulations with the simpler model used by van der Schrier et al. (2002), that sea level reconstructions from Connecticut reflect variations in the deep-ocean geopotential height. They compare a small ensemble of similar simulations to sea level reconstructions from Connecticut and explain the observed lag between solar forcing and sea level reconstruction with the slow transport of deep-ocean geopotential height anomalies by the meridional overturning circulation. This yields a lag comparable to the one observed in the data. Furthermore, simulated and reconstructed Connecticut sea level have a similar temporal response.

A further analysis of local SL variations shows widely different mechanisms for the different areas in the North Atlantic in the current simulation.

Along the Atlantic seaboard of the southeastern United States, steric sea level variations at the multidecadal/centennial time scale are largely related to variations in the divergence of meridional heat transport. Meridional advection of heat appears to be stronger related to the gyre circulation than to the meridional overturning circulation just off the eastern Atlantic seaboard of the United States, whereas the reverse is the case farther offshore. Moreover, variations in sea level in this region cannot be explained by steric sea level variations only, variations in gyre circulation are reflected in SL too. Divergences in the advective heat flux are larger than the ocean–atmosphere heat flux along the Gulf Stream, but in the stagnant water masses of the subtropical North Atlantic, the surface flux dominates ocean heat content variability.

Multidecadal/centennial sea level variability in the slope water region is not related to the strength of the Gulf Stream but is for a large part related to north- and southward shifts in its position, bringing this region under the influence of alternating phases of cold subpolar or warm subtropical water. This suggests that the sea level reconstructions from the Gulf of Maine (Gehrels et al., 2003) and Long Island Sound (van de Plassche, 2000) reflect variations in the position of the Gulf Stream. Typical centennial variations in reconstructed sea level from Machiasport and Wells (Maine) (Gehrels, 1999; Gehrels et al., 2002) are 4–10 cm, which is comparable to the typical variations in the 100 year low-pass-filtered model data of 4–6 cm. The interpretation of Fletcher et al. (1993) of their SL reconstruction for Wolf Glade (Delaware), in terms of variations of the Gulf Stream, is thus closest to what the model data show.

Finally, sea level in the Labrador Sea, especially along the western margin, seems to be related both to changes in the hydrography and to changes in the wind-driven circulation. Farther offshore, sea level seems to be related to the meridional overturning circulation, with highest correlations in the central subpolar gyre, extending to the northern parts of the Labrador Sea.

Keigwin and Pickart (1999) found evidence of a dipole in sea-surface temperature (SST). Based on planktonic foraminiferal analysis, they argue that changes in the SSTs over the Laurentian Fan (situated 42°N–45°N, 57°W–54°W) on centennial/millennial time scales were out of phase with those from the Bermuda Rise in the Sargasso Sea (Keigwin, 1996). Changes in SST on the Laurentian fan were subsequently related to the north- and southward shifting of (a branch of) the Gulf Stream. This dipole structure is also retrieved in the current simulation in geopotential height of the upper 535 m, where one center of the dipole correlates -0.6 with the other and vice versa.

However, the influence of the north- and southward shifts of the Gulf Stream on SST in the Laurentian Fan region is less obvious. A correlation (40 years, low-pass-filtered) between the second principal component of sea level (indicating the north/southward shifting) and SST gives positive but modest correlations in this region (0.2, 0.3), which fail to be statistically significant. Furthermore, Keigwin and Pickart (1999) argue that the slope water system oscillates in phase with the North Atlantic Oscillation (NAO). The data analysed here indicate only a weak link between the two; a correlation (40 years, low-pass-filtered and at lag 0) between the NAO index [as defined by Cooper and Gordon (2002)] and the position of the Gulf Stream gives 0.36, which is just barely significant at the 95% level.

Battisti et al. (1995) hindcast North Atlantic winter SSTs using a model with a mixed layer excluding any circulation, atop a diffusive deep ocean. The model was forced by ocean–atmosphere heat fluxes derived from observed fields and simulated rather successfully SST in large areas of the North Atlantic. This suggests that the ocean merely integrates atmospheric forcing with a response having more energy at low frequencies than at higher frequencies. This mechanism is not identified in the current analysis of low-frequency steric sea level along the eastern seaboard of the United States and in the strong advective regimes of the Gulf Stream/NAC system. On the multidecadal/centennial time scale, heat flux variability paces heat content only in the stagnant water masses of the subtropical gyre.

Although the HadCM3 model is a state-of-the-art model, generally thought to be superior to a host of other GCMs, Gordon et al. (2000) note that with a horizontal resolution of $1.25° \times 1.25°$, the degree or realistic behaviour in western boundary currents as the Gulf Stream still leaves something to be desired. This observation could make some differences in the conclusions of this study.

The data analysed here are from a control simulation. Any fluctuations in climate originating from variations in external sources as solar activity, volcanism and greenhouse gasses are not included. Taking variations in these forcing agents into account might modify present conclusions. The analysis of a 500-year HadCM3 experiment using solar and volcanic forcings, which is currently being conducted, would contribute to this matter. However, an earlier analysis (van der Schrier et al., 2002) using a simpler model suggests that the same mechanisms of multidecadal/centennial sea level change are found in both the control simulation and a simulation forced by solar irradiance changes. However, the amplitude of sea level variations in the latter simulation was observed to be significantly larger.

Present analysis has shown the complex nature of regional SL variations at the multidecadal/centennial time scale in the North Atlantic. This complexity has consequences for the interpretation of multidecadal/centennial variability in SL reconstructions.

Acknowledgements

We would like to thank Dr. J. M. Gregory, Dr. G. Lohmann, Prof. D.F. Belknap and Prof. P. Wu for their constructive suggestions.

Appendix A. Computation of sea level in HadCM3

The computation of sea level in HadCM3 (and other models) is exhaustively dealt with by Gregory et al. (2001). Here, a summary is given.

Sea level in the HadCM3 model needs to be computed diagnostically from model output, because the ocean component of HadCM3 is a rigid-lid ocean where the sea surface topography is reflected in pressure variations exerted by the lid. The rigid-lid pressure p_s can be converted to sea-surface height by using the hydrostatic equation:

$$p_s = \eta \rho_* g, \tag{A1}$$

where η is the relative topography, ρ_* the density of sea water at the surface and g the acceleration due to gravity. The rigid-lid pressure gradient $\nabla_h p_s$ enters the momentum equation, and the vertically averaged momentum equation is:

$$\frac{1}{H}\int_{-H}^{0}\frac{\partial \mathbf{u}_H}{\partial t}\mathrm{d}z = \frac{1}{H}\int_{-H}^{0}\mathbf{F}\mathrm{d}z - \frac{1}{\rho_0}\nabla_h p_s, \tag{A2}$$

where $\mathbf{u}_H$ is the horizontal velocity, $\mathbf{F}$ the aggregate of all forcing terms in the momentum equations (excluding the rigid-lid pressure gradient) and ρ_0 a nominal

density. Because the flow is nondivergent, it can be represented by a stream function ψ, leading to:

$$\frac{1}{\rho_0}\nabla_h p_s = \frac{1}{H}\int_{-H}^{0}\mathbf{F}\mathrm{d}z - \frac{1}{H}\mathbf{k}\times\nabla_h\frac{\partial\psi}{\partial t}, \qquad \text{(A3)}$$

where $\mathbf{k}$ is the vertical unit vector. The relative topography η is computed by evaluating the right hand side of (A3) from the model, which gives $\nabla_h p_s$, and then extracting p_s by a numerical minimisation. Finally, η is computed using (A1).

References

Battisti, D.S., Bhatt, U.S., Alexander, M.A., 1995. A modelling study of the interannual variability in the wintertime North Atlantic Ocean. J. Climate 8, 3067–3083.

Charnock, H., 1994. Air–sea exchanges and meridional fluxes. In: Malanotti-Rizzoli, P., Robinson, A.R. (Eds.), Ocean Processes in Climate Dynamics: Global and Mediterranean Examples. Kluwer Academic Publishing, pp. 1–27.

Church, J.A., Gregory, J.M., Huybrechts, P., Kuhn, M., Lambeck, K., Nhuan, M.T., Qin, D., Woodworth, P.L., 2001. Changes in sea level. In: Houghton, J.T., et al. (Eds.), Climate Change 2001: The Scientific Basis. Contribution of Working Group I to the Third Assessment Report of the Intergovernmental Panel on Climate Change. Cambridge Univ. Press, pp. 639–693. Chapt. 11.

Cooper, C., Gordon, C., 2002. North Atlantic decadal variability in the Hadley Centre coupled model. J. Climate 15, 45–72.

Crowley, T.J., Baum, S.K., Kim, K.-Y., Hegerl, G.C., Hyde, W.T., 2003. Modelling ocean heat content changes during the last millennium. Geophys. Res. Lett. 30 (18) CLM3 (doi:10.1029/2003GL017801).

Curry, R.G., McCartney, M.S., 2001. Ocean gyre circulation changes associated with the North Atlantic oscillation. J. Phys. Oceanogr. 31, 3374–3400.

Flament, P., 2002. A state variable for characterizing water masses and their diffusive stability: spiciness. Prog. Oceanogr. 54, 493–501.

Fletcher, C.H., Van Pelt, J.E., Brush, G.S., Sherman, J., 1993. Tidal wetland record of Holocene sea-level movements and climate history. Palaeogeogr. Palaeoclimatol. Palaeoecol. 102, 177–213.

Gehrels, W.R., 1999. Middle and late Holocene sea-level changes in eastern Maine reconstructed from foraminiferal saltmarsh stratigraphy and AMS ^{14}C dates on basal peat. Quat. Res. 52, 350–359.

Gehrels, W.R., Belknap, D.F., Black, S., Newnham, R.M., 2002. Rapid sea-level rise in the Gulf of Maine, USA, since AD 1800. Holocene 12, 383–390.

Gehrels, W.R., Newnham, R.M., Kirby, J.R., Black, S., Truscott, J.B., 2003. Sea-level changes in the western Atlantic during the past 300 years. Geophysical Research Abstracts, vol. 5. European Geophysical Society, Kadenberg-Lindace, Abstract 01245.

Gordon, C., Cooper, C., Senior, C.A., Banks, H., Gregory, J.M., Johns, T.C., Mitchell, J.F.B., Wood, R.A., 2000. The simulation of SST, sea ice extents and ocean heat transports in a version of the Hadley Centre coupled model without flux correction. Clim. Dyn. 16, 147–168.

Gregory, J.M., Church, J.A., Boer, G.J., Dixon, K.W., Flato, G.M., Jackett, D.R., Lowe, J.A., O'Farall, S.P., Roeckner, E., Russell, G.L., 2001. Comparison of results from several AOGCMs for global and regional sea-level change 1900–2100. Clim. Dyn. 18, 225–240.

Houghton, R.W., Visbeck, M.H., 2002. Quasi-decadal salinity fluctuations in the Labrador Sea. J. Phys. Oceanogr. 32, 687–701.

Keigwin, L.D., 1996. The little ice age and medieval warm period in the Sargasso Sea. Science 274, 1504–1508.

Keigwin, L.D., Pickart, R.S., 1999. Slope water current over the laurentide fan on interannual to millenial time scales. Science 286, 520–523.

Levitus, S., 1990. Interpentadal variability of steric sea level and geopotential thickness on the North Atlantic Ocean, 1970–1974 versus 1955–1959. J. Geophys. Res. (Oceans) 95, 5233–5238.

Long, A., 2000. Late Holocene sea-level change and climate. Prog. Phys. Geogr. 24, 415–423.

Noble, M.A., Gelfenbaum, G.R., 1992. Seasonal fluctuations in sea level on the south Carolina shelf and their relationship to the Gulf Stream. J. Geophys. Res. (Oceans) 97, 9521–9529.

Pope, V.D., Gallani, M.L., Rowntree, P.R., Stratton, R.A., 2000. The impact of new physical parametrizations in the Hadley Centre climate model: HadAM3. Clim. Dyn. 16, 123–146.

Saenko, O.A., Gregory, J.M., Weaver, A.J., Eby, M., 2002. Distinguishing the influence of heat, freshwater, and momentum fluxes on ocean circulation and climate. J. Climate 15, 3686–3696.

Schmitt, R.W., Bogden, P.S., Dorman, C.E., 1989. Evaporation minus precipitation and density fluxes for the North Atlantic. J. Phys. Oceanogr. 19, 1208–1221.

van de Plassche, O., 2000. North Atlantic climate–ocean variations and sea-level in Long Island Sound, Connecticut, Since 500 cal yr AD. Quat. Res. 53, 89–97.

van de Plassche, O., van der Schrier, G., Weber, S.L., Gehrels, W.R., Wright, A.J., 2003. Sea-level variability in the northwest Atlantic during the past 1500 years: a delayed response to solar forcing? Geophys. Res. Lett. 30 (18), 1921 (doi:10.1029/2003GL017558).

van der Schrier, G., Weber, S.L., Drijfhout, S.S., 2002. Sea level changes in the North Atlantic by solar forcing and internal variability. Clim. Dyn. 19, 435–447.

Vellinga, M., Wu, P. Natural variability of the Atlantic thermohaline circulation in HadCM3. J. Climate (submitted for publication).